PROCEEDINGS OF SCIENCE

Neutral current quasielastic (anti)neutrino scattering beyond the Fermi gas model at MiniBooNE and BNL kinematics

M.V. Ivanov,[a,*] **A.N. Antonov,**[a] **M.B. Barbaro,**[b,c] **C. Giusti,**[d] **A. Meucci,**[d] **J.A. Caballero,**[e] **R. González-Jiménez,**[f] **E. Moya de Guerra**[f] **and J.M. Udías**[f]

[a] *Institute for Nuclear Research and Nuclear Energy, Bulgarian Academy of Sciences, Sofia 1784, Bulgaria*

[b] *Dipartimento di Fisica dell'Università di Torino and INFN – Sezione di Torino, via Pietro Giuria 1, 10125 Turin, Italy*

[c] *Université Paris-Saclay, CNRS/IN2P3, IJCLab, 15 rue Georges Clémenceau, 91405 Orsay cedex, France*

[d] *Dipartimento di Fisica, Università degli Studi di Pavia and INFN – Sezione di Pavia, via Bassi 6 I-27100 Pavia, Italy*

[e] *Departamento de Física Atómica, Molecular y Nuclear, Universidad de Sevilla, 41080 Sevilla, Spain*

[f] *Grupo de Física Nuclear, Departamento de Estructura de la Materia, Física Térmica y Electrónica, Facultad de Ciencias Físicas, Universidad Complutense de Madrid and IPARCOS, CEI Moncloa, Madrid 28040, Spain*

E-mail: martin@inrne.bas.bg

Neutral current quasielastic (anti)neutrino scattering cross sections on a ^{12}C target are analyzed using a realistic spectral function $S(p, \mathcal{E})$ that gives a scaling function in accordance with the (e, e') scattering data. The spectral function accounts for the nucleon-nucleon (NN) correlations by using natural orbitals from the Jastrow correlation method and has a realistic energy dependence. The standard value of the axial mass $M_A = 1.03$ GeV is used in all calculations. The role of the final-state interaction on the spectral and scaling functions, as well as on the cross sections is accounted for. A comparison of the calculations with the empirical data of the MiniBooNE and BNL experiments is performed. Our results are analyzed in comparison with those when NN correlations are not included, and also with results from other theoretical approaches, such as the relativistic Fermi gas, the relativistic mean field, the relativistic Green's function, as well as with the superscaling approach based on the analysis of quasielastic electron scattering.

11th International Conference of the Balkan Physical Union (BPU11),
28 August - 1 September 2022
Belgrade, Serbia

*Speaker

PoS(BPU11)017

1. Introduction

The analysis of neutrino oscillations is at present one of the main research topics in Physics. This explains the huge activity in the field and the numerous experiments that have been proposed in several facilities and covering a very wide range in energy. For the first time, experimental data on neutrino interactions are being measured with a high statistics and small error bands. As a consequence, a great variety of studies on the theoretical side have also appeared trying to describe the data. These include analyses from low-to-intermediate energies where the nuclear effects may play an important role, to very high energies where the nucleonic and/or subnucleonic degrees of freedom are the principal ingredientes. In all cases, the understanding of neutrino properties is a key ingredient in elementary particle physics.

Our interest in the present work concerns the analysis of different experimental data recently obtained on neutrino-nucleus processes in several facilities. At around 1 GeV, data are available from the MiniBooNE collaboration, both for charged-current (CC) [1] and neutral current (NC) [2] ν–^{12}C processes, and prevail all previous experiments [3]. We note also that recent data for $\bar{\nu}$–nucleus scattering are reported in [4, 5]. As known, the analyses of nuclear effects in neutrino scattering are generally regarded as one of the main sources of systematic uncertainties in oscillation experiments, in particular, when it concerns the understanding of charged-current quasielastic (CCQE) interaction with nucleons bound in the nucleus (*e.g.* [6]) in the energy range of around 1 GeV. For energies of a few GeV, the Δ-resonance excitation becomes equally important [7].

Though the main subject of our work is the neutral current QE neutrino scattering by nuclei, in what follows we would like to note various theoretical models that have been used also for the description of CC processes in connection to their applications to analyses of the NC processes.

The analyses of the CCQE MiniBooNE data have raised questions on the capabilities of the various models to account for the different contributions to the neutrino-nucleus scattering cross sections. The relativistic Fermi gas (RFG) model, in which the shell structure and the nucleon correlations are neglected, gives results for the CCQE neutrino scattering that underestimate the data. The accordance with the data is achieved by increasing the world-average axial mass M_A ($M_A = 1.03$ GeV) to $M_A = 1.35$ GeV. An enhancement of the world-average axial mass is required also in other models based on the impulse approximation (IA) (*e.g.* [6, 8–15]). This is an indication that models based on the IA may lack important contributions to the processes of neutrino-nucleus scattering. In approaches beyond the IA, ingredients such as two-particle two-hole ($2p-2h$) contributions have been included. In the works [16, 17] an approach based on the random-phase approximation, improved by considering relativistic corrections [11] led to a good agreement with the MiniBooNE data for both CCQE and neutral current quasielastic (NCQE) scattering, including the double differential CCQE cross section. It was pointed out in [12] that the multinucleon contribution may effectively be accounted for by increasing the value of the axial mass. As shown in [13, 18–20], the relativistic mean field (RMF) approach gives a good description of the shape of the double differential cross section from the MiniBooNE experiment but fails to reproduce its normalization. It has been noted in [13] that meson exchange currents (MEC) could reduce the discrepancy. The calculations within the relativistic Green's function (RGF) model [8, 21, 22] have provided a good description of the total CCQE and of the (double) differential (CCQE) NCQE MiniBooNE cross sections [8, 14, 18, 21, 23]. The larger RGF cross sections can be attributed

to the overall effect of inelastic channels, such as, for instance, rescattering of the knocked-out nucleon, multinucleon processes, non-nucleonic Δ-excitation, that are recovered in the model by the use of a complex relativistic optical potential to describe final state interaction (FSI) and that are not included in other models based on the IA.

For a detailed discussion of the scaling and superscaling models, the reader is referred to [24–37]. The analysis of CC (anti)neutrino scattering with no pions in the final state (denoted as CC0π) has proven the essential role played by two-particle two-hole (2p-2h) Meson Exchange Currents (MEC) in addition to the quasielastic (QE) response. The inclusion of these two contributions has allowed one to explain data for different experiments without the need to modify the standard value of the axial mass M_A [12, 16, 38–40]. It is important to point out that, contrary to the electron scattering, in (anti)neutrino-nucleus processes the neutrino energy is not known precisely, and this implies that one- and two-body responses cannot be disentangled in the inclusive experimental data, where only the outgoing lepton is detected.

In parallel, it is also interesting to compare with the older NCQE data from the Brookhaven BNL E734 experiment [41], corresponding to neutrino kinematics similar to MiniBooNE. We should emphasize that the NC cross sections depend also on the strangeness content of the nucleon, particularly, through the axial form factor. Hence a good control of nuclear effects is also required if one wants to extract information on the strange form factors of the nucleon from NC data.

The main aim of this paper is to analyze neutral current QE (anti)neutrino scattering cross sections on a ^{12}C target using a realistic spectral function $S(p, \mathcal{E})$ that gives a scaling function in accordance with the (e, e') scattering data. In our works [42, 43] this approach was applied to calculate CCQE (anti)neutrino scattering on ^{12}C. The spectral function accounts for the NN correlations by using natural orbitals (NO's) from the Jastrow correlation method and has a realistic energy dependence. In the calculations the standard value of the axial mass $M_A = 1.03$ GeV is used and the role of FSI on the scaling functions and on the cross sections is taken into account. A comparison of the calculations with the empirical data of the MiniBooNE and BNL experiments is performed.

2. Theoretical Scheme

The general formalism for NC (anti)neutrino scattering in the QE regime has been introduced in many previous works [44–49]. Here we summarize briefly those aspects which are of more relevance for the later discussion of the results and of their comparison with MiniBooNE and BNL data. We consider the semi-leptonic quasi-free scattering from nuclei in Born approximation, assuming that the inclusive cross sections are well represented by the sum of the integrated semi-inclusive proton and neutron emission cross sections [44]. The kinematics for semi-leptonic nucleon knockout reactions in the one-boson-exchange approximation is presented in Figure 1.

A lepton with 4-momentum $K^\mu = (\epsilon, \mathbf{k})$ scatters to another lepton with 4-momentum $K'^\mu = (\epsilon', \mathbf{k}')$, exchanging a vector boson with 4-momentum $Q^\mu = K^\mu - K'^\mu$. The lepton energies are $\epsilon = \sqrt{m^2 + k^2}$ and $\epsilon' = \sqrt{m'^2 + k'^2}$, where the masses of the initial and final lepton m and m' are assumed to be equal to zero for NC neutrino scattering. In the laboratory system the initial nucleus being in its ground state has a 4-momentum $P_A^\mu = (M_A^0, 0)$, while the final hadronic state corresponds to a proton or neutron with 4-momentum $P^\mu_{N=p \text{ or } n} = (E_N, \mathbf{p}_N)$ and an unobserved

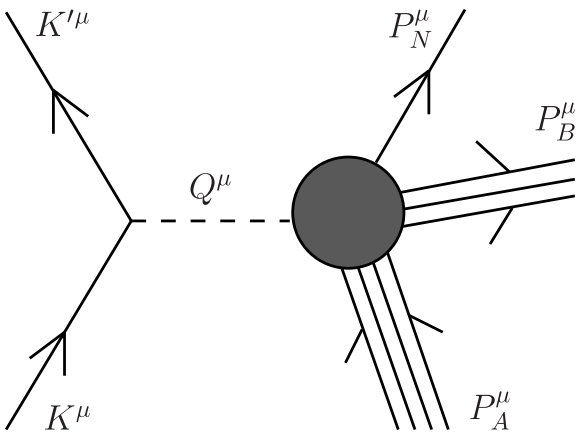

Figure 1: Kinematics for semi-leptonic nucleon knockout reactions in the one-boson-exchange approximation.

residual nucleus with 4-momentum $P_B^{\mu} = (E_B, \mathbf{p}_B)$. Usually the missing momentum $\mathbf{p} \equiv -\mathbf{p}_B$ and the excitation energy $\mathcal{E} \equiv E_B - E_B^0$, with $E_B^0 = \sqrt{\left(M_B^0\right)^2 + p^2}$ are introduced, M_B^0 being the ground-state mass of the daughter nucleus. Although in real situations, as is the case for MiniBooNE and BNL, there are usually no monochromatic beams and an integral over the allowed energies folded with the neutrino flux must be performed, we assume the energy of the incident neutrino to be specified and also the outgoing nucleon energy E_N to be known. Finally, the angle θ_{kp_N} between the incident neutrino and the ejected nucleon momentum is also given.

Starting from the Feynman amplitude associated with the exclusive diagram of Figure 1, one can get inclusive cross sections by integrating over the undetected outgoing particles.

In the case of QE electron- or CCQE neutrino-scattering, the outgoing lepton is detected and a sum over the outgoing nucleon variables is performed. Using the language introduced in this context in Ref. [46], we refer to these processes as "t-channel" reactions, since the Mandelstam variable $t = (K^{\mu} - K'^{\mu})^2$ is fixed. Then the (e, e') and CC (ν_l, l') reactions are governed by the same kinematics and the scaling formalism developed for the former can be trivially extended to the latter.

In the case of NC neutrino scattering only the outgoing nucleon can be experimentally detected, while the unobserved outgoing neutrino is integrated over. This is referred to as a "u-channel" process, where the Mandelstam variable $u = (K^{\mu} - P^{\mu})^2$ is fixed. Then the kinematics is not the same as in the (e, e') case and, in particular, the two inclusive cross sections involve an integration over a slightly different region in the missing energy and momentum plane. As a consequence it is not evident that the scaling arguments can be applied to NC scattering. However, in [44] the influence of a non-constant Q^{μ} in the derivation of scaling in the NC case was thoroughly investigated within the general framework of the RFG model concluding that the scaling ideas still work properly for NC neutrino-nucleus processes. That study was extended in [48, 51] making use of the RMF approach. These results showed that scaling of the second kind, *i.e.,* independence of the nuclear target, works extremely well. On the contrary, scaling of first kind (independence on the transfer momentum) depends on the specific kinematical situation considered. In general, first-kind scaling seems to be well respected when the angle of the ejected nucleon is larger than

roughly 50°. This is the region where the cross section integrated over angles reaches larger values. Therefore, first-kind scaling is expected to work properly at MiniBooNE and BNL. Indeed, for the RMF and the particular kinematics involved in the experiments analyzed in this work (MiniBooNE and BNL), we have verified that the calculation of the NC cross sections based on u-scaling gives rise to results very similar (within few percents) to those provided by the full calculation, *i.e.,* without resorting to the scaling assumption. This is strictly true for $Q^2 \lesssim 0.7$ GeV^2. For larger values of Q^2, the u-scaling approximation begins to deviate from the full result, but by an amount significantly smaller than the uncertainty linked to the data error bands.

The usual procedure for calculating the $(l, l'N)$ cross section includes the Plane Wave Impulse Approximation (PWIA) and integrations over all unconstrained kinematic variables. It is shown in [44] that the inclusive cross section in the u-channel can be written after some approximations in the following form:

$$\frac{d\sigma}{d\Omega_N dp_N} \simeq \overline{\sigma}^{(u)}_{s.n.} F(y', q'), \tag{1}$$

where

$$F(y', q') \equiv \int_{\mathcal{D}_u} p dp \int \frac{d\mathcal{E}}{E} \Sigma \simeq F(y'), \tag{2}$$

provided the effective NC single nucleon (s.n.) cross section

$$\overline{\sigma}^{(u)}_{\text{s.n.}} = \frac{1}{32\pi\epsilon} \frac{1}{q'} \left(\frac{p_N^2}{E_N} \right) g^4 \int_0^{2\pi} \frac{d\phi'}{2\pi} l_{\mu\nu}(\mathbf{k}, \mathbf{k}') w^{\mu\nu}(\mathbf{p}, \mathbf{p}_N) D_V (Q^2)^2 \tag{3}$$

is almost independent of $(p, \mathcal{E})$ for constant (k, p_N, θ_{kp_N}). In Eq. (3) $l_{\mu\nu}$ and $w^{\mu\nu}$ are the leptonic and s.n. hadronic tensor, respectively, and $D_V (Q^2)$ is the vector boson propagator [44]. Eqs. (1)–(3) contain $Q'^{\mu} \equiv K^{\mu} - P_N^{\mu} = (\omega', \mathbf{q}')$ that is the four-momentum transferred from the initial lepton to the ejected nucleon and y' is the scaling variable naturally arising in the u-scattering kinematics, analogous to the usual y-scaling variable for t-scattering. The scaling function $F(y')$ obtained within a given approach can be used to predict realistic NC cross sections. Assuming that the domains of integration $\mathcal{D}_u$ (in the u-channel) and $\mathcal{D}_t$ (in the t-channel) are the same or very similar, the results for the scaling function obtained in the case of inclusive electron scattering (where $\mathcal{D}_t$ works) can be used in the case of NC neutrino reactions. It is pointed out in [44] that $\mathcal{D}_t$ and $\mathcal{D}_u$ differ significantly only at large $\mathcal{E}$ (also at large p, but there the semi-inclusive cross sections are expected to be negligible). So, given that the semi-inclusive cross sections are dominated by their behavior at low $\mathcal{E}$ and low p, one expects the results of the integrations in the t- and u-channel to be very similar, and thus the scaling functions will be essentially the same in both cases.

In this work we use in the calculations the RFG, superscaling approach (SuSA), harmonic oscillator (HO+FSI) and natural orbitals (NO+FSI) scaling functions including final state interactions (see Refs. [42, 50]). We present also results obtained in the RMF and RGF models, where the cross sections are calculated in a fully unfactorized approach which does not make use of the approximations leading to Eq. (1). All our results are used to analyze NCQE (anti)neutrino cross sections on a CH_2 target measured by the MiniBooNE collaboration [2, 5]. We shall also compare with the BNL E734 experiment [41], studying νp and $\bar{\nu} p$ NCQE interactions, where the target was composed in 79% of protons bound in carbon and aluminum and in 21% of free protons.

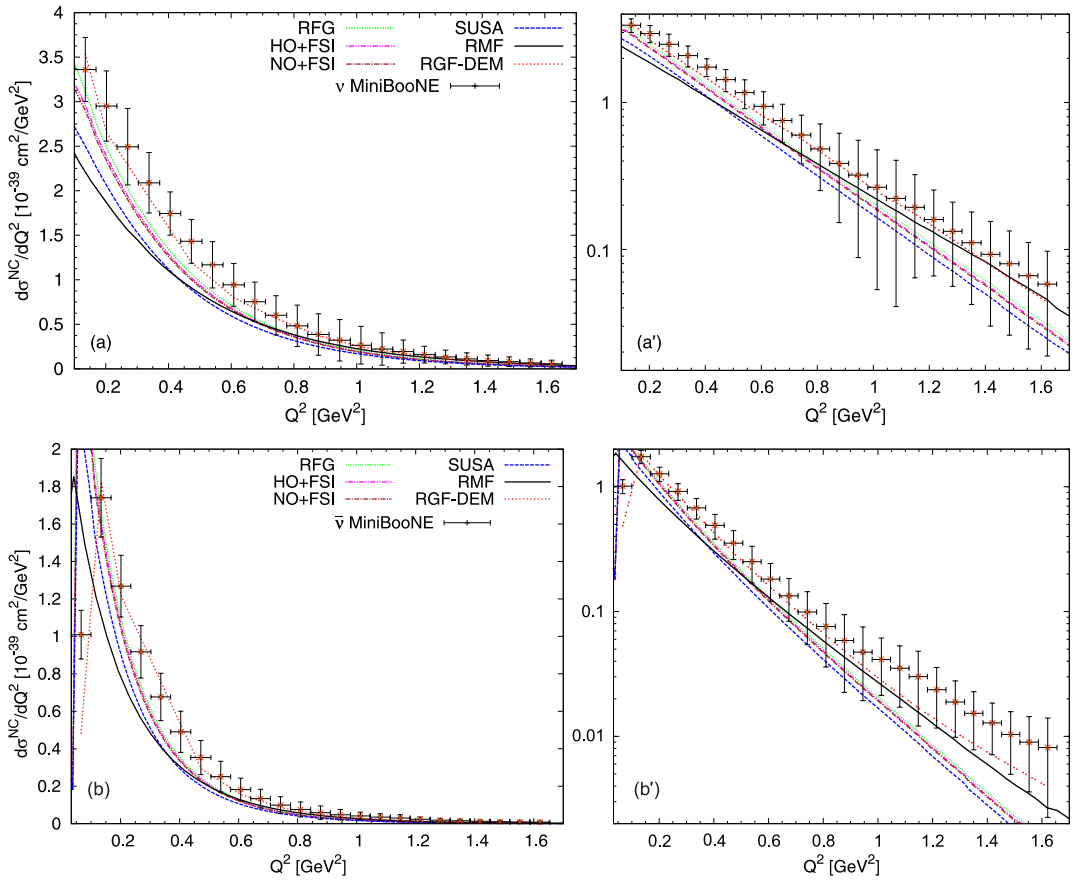

Figure 2: NCQE neutrino [panels (a) and (a′), $\nu N \to \nu N$] and antineutrino [panels (b) and (b′), $\bar{\nu} N \to \bar{\nu} N$] flux-averaged differential cross section computed using the RFG, HO+FSI, NO+FSI, SUSA scaling functions, RGF and RMF models and compared with the MiniBooNE data [2, 5]. The results correspond to the world-average axial mass $M_A = 1.03$ GeV and strangeness $\Delta s = 0$. The error bars do not account for the normalization uncertainty of 18.1% (19.5%) in the $\nu(\bar{\nu})$ case.

3. Results and Discussion

In this section the theoretical predictions of the RFG, HO+FSI, NO+FSI, SUSA scaling functions are compared with the data measured by the MiniBooNE and BNL Collaborations. The comparison is performed also with the results of the RMF and RGF models, which are based on the same relativistic mean-field model for nuclear structure but on a different treatment of FSI. In the RMF model FSI are described by the same relativistic mean field potential describing the initial nucleon state. The description of FSI in the RGF is based on the use of a complex optical potential. Details of the RGF model can be found, for instance, in [52, 53]. The results of the RMF and RGF models have been already and widely compared in [22] for the inclusive QE electron scattering, in [14, 54] for CCQE and in [18] for NCQE neutrino scattering. The RGF calculations presented in this work have been carried out with the so-called "democratic" parametrization of the optical potential of [55] (RGF-DEM).

The comparison between theory and experiment for the NCQE flux-averaged MiniBooNE (anti)neutrino cross section is presented in Figure 2. Here we compare the predictions obtained by the usage of the RFG, HO+FSI, NO+FSI, SUSA scaling functions, and RMF model with the data.

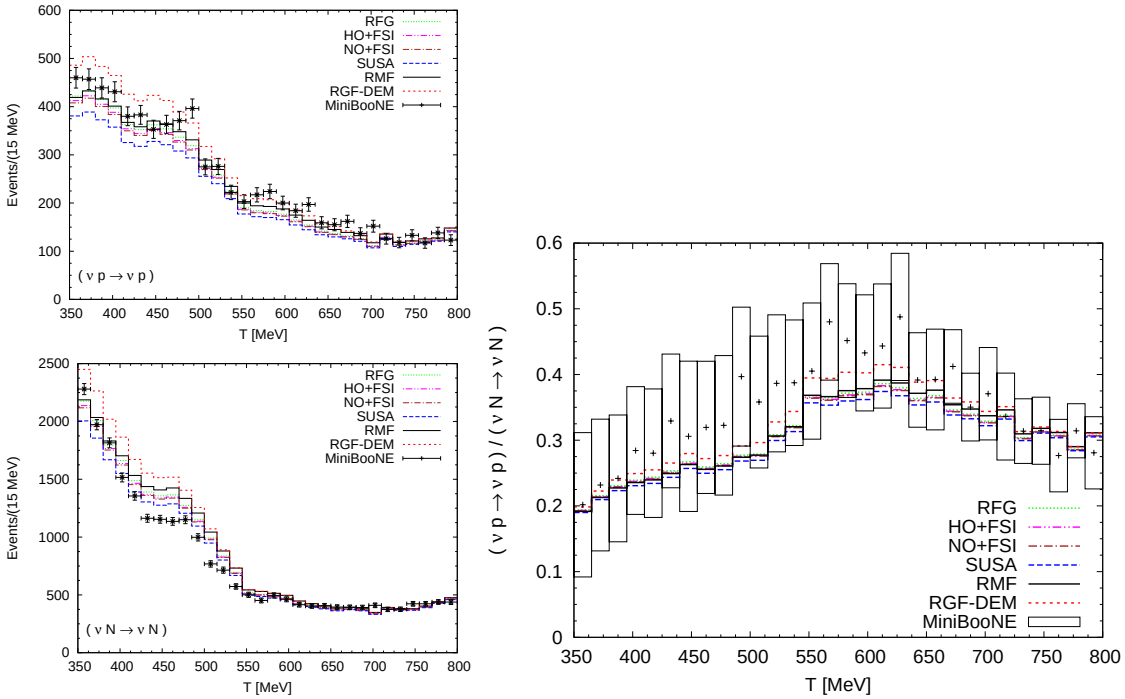

Figure 3: The RFG, HO+FSI, NO+FSI, SUSA, RGF, and RMF predictions, after the folding procedure, compared with the histograms of the numerator (top-left panel) and denominator (bottom-left panel) of the ratio. The error bars in the left panel represent only the statistical uncertainty, computed as the square root of the event number. The corresponding ratio is shown in the right panel of the figure. The axial mass and strangeness have been assumed to be the standard axial mass value and zero strangeness. Data are taken from [2, 56, 57].

As usually in NC reactions, in this work, the variable Q^2 is defined as $Q^2 = 2M_N T_N$, where M_N and T_N are the mass and kinetic energy of the outgoing nucleon, respectively. As can be seen from Figure 2 the theoretical results corresponding to all models except the RGF-DEM underestimate the neutrino data in the region between $0.1 < Q^2 < 0.7$ GeV^2, while all theories are within the error bars for higher Q^2. On the other hand the same models underestimate the antineutrino data at high Q^2. This is clearly seen in the panels (a′) and (b′) of Figure 2, where the cross sections are represented in logarithmic scale. The RGF-DEM results are larger than the results of the other models and in generally good agreement with the data over the entire Q^2 region considered in the figure. The enhancement of the RGF cross sections is due to the contribution of final-state channels that are recovered by the imaginary part of the optical potential and are not included in the other models.

We present in Figure 3 the spectra corresponding to the numerator and denominator entering the ratio between ν-scattering from proton and nucleon (proton plus neutron) (left panels) and the ratio computed by dividing of the two samples (right panels) within the various models and compared with the MiniBooNE data [2]. The numerator and denominator data (left panels of Figure 3) are taken from [57], where the data are reported without the corresponding errors (so, in the figure only statistical errors are included). In the calculations the axial mass (M_A) and strangeness (Δs) have been assumed to be the standard axial mass and zero strangeness. We note that the dispersion between the models tends to cancel when this ratio is considered. This result clearly shows that the

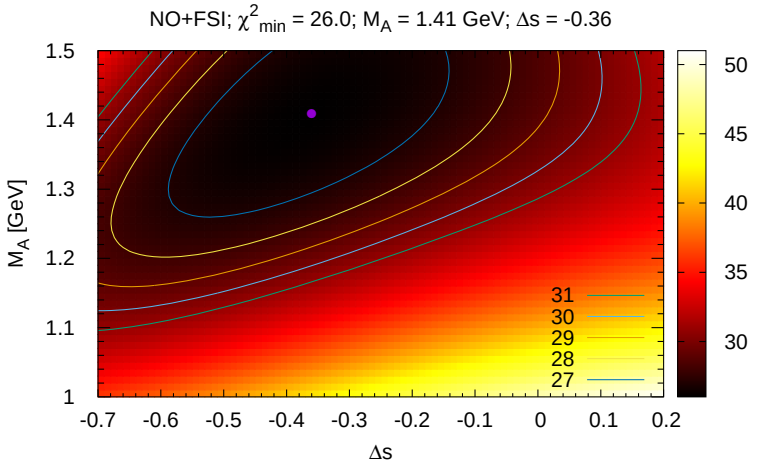

Figure 4: Results of the M_A and Δs fit of the NO+FSI model to the MiniBooNE NCQE *reconstructed* cross section data [57]. The χ^2 values are for 49 DOF. The minimum is located at $M_A = 1.41$ GeV, $\Delta s = -0.36$.

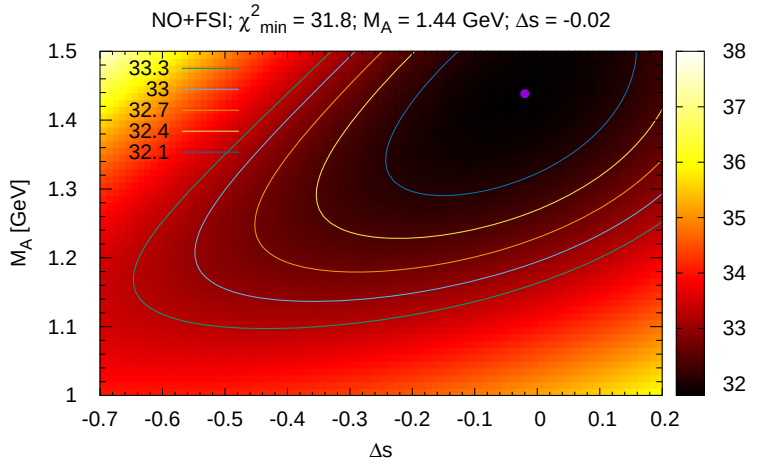

Figure 5: Results of the M_A and Δs fit of the NO+FSI model to the MiniBooNE NCQE *reconstructed* $(\nu_\mu p \to \nu_\mu p)/(\nu_\mu N \to \nu_\mu N)$ data [57]. The χ^2 values are for 28 DOF. The minimum is located at $M_A = 1.44$ GeV, $\Delta s = -0.02$.

proton/nucleon ratio is very insensitive to nuclear model effects and to final state interactions, and hence, it may provide information that improves our present knowledge on the electroweak nucleon structure, in particular, the nucleon's strangeness. In particular, for kinetic energies of the outgoing nucleon $T_N > 350$ MeV our models give results which are in good agreement with the experimental data (left panels of Figure 3), while for the ratio our theoretical results are within the error bars at all kinematics (right panel of Figure 3).

For completeness, a study of $\chi^2(M_A, \Delta s)$ using the *reconstructed* energy distribution for the cross section and the $(\nu_\mu p \to \nu_\mu p)/(\nu_\mu N \to \nu_\mu N)$ ratio has been done within NO+FSI model. In this work we extend the previous analysis by performing a combined fit procedure that takes simultaneously the role played by M_A and Δs, assuming $M_A = 1.03$ GeV for free protons. We use the definition of χ^2 given in Appendix B5 of Ref. [56] and corresponding error matrices for the NCQE sample and the $(\nu_\mu p \to \nu_\mu p)/(\nu_\mu N \to \nu_\mu N)$ ratio [57]. The results are presented in Figures 4 and 5. We show in two cases the absolute minimum of $\chi^2(M_A, \Delta s)$ and the corresponding

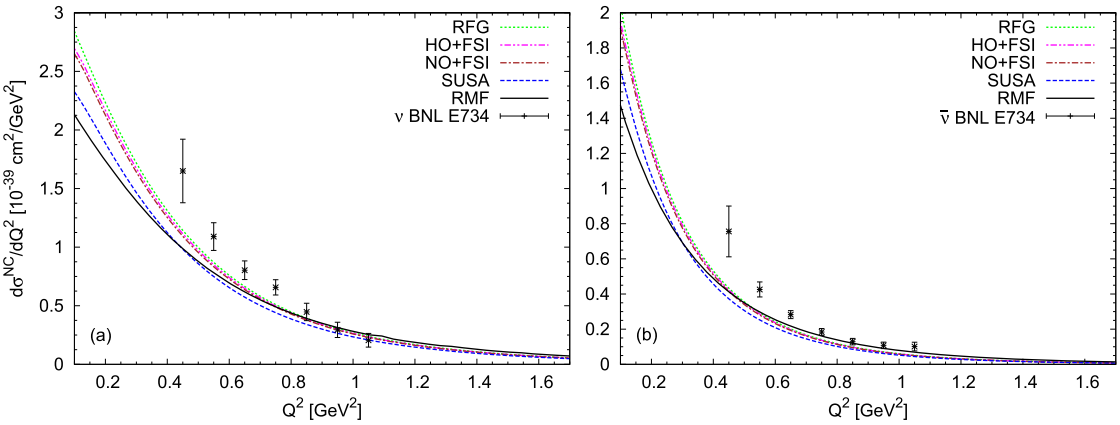

Figure 6: NCQE flux-averaged cross section: $\nu p \to \nu p$ [panel (a)] and $\bar{\nu} p \to \bar{\nu} p$ [panel (b)] compared with the BNL E734 experimental data [41]. Our results are evaluated using the RFG, HO+FSI, NO+FSI, SUSA scaling functions, and RMF model with the standard value of the axial-vector dipole mass $M_A = 1.03$ GeV^2 and strangeness $\Delta s = 0$. The error bars do not include the normalization uncertainty of 11.2% (10.4%) in the $\nu(\bar{\nu})$ case.

1σ ellipses. The absolute χ^2 minima within NO+FSI model are obtained at ($M_A = 1.41$ GeV, $\Delta s = -0.36$) for the *reconstructed* cross section data and ($M_A = 1.44$ GeV, $g_A^{(s)} = -0.02$) for the $(\nu_\mu p \to \nu_\mu p)/(\nu_\mu N \to \nu_\mu N)$ ratio data. The location of the minima is almost constant against the axial mass. However, great caution should be drawn to the results because of the extremely large (negative) values of the axial strangeness, which correspond to very suppressed neutrons contribution to the NCQE cross section. In fact, these values are not consistent with the results provided by the BNL E734 experiment [41] which measured the value $\Delta s = -0.15 \pm 0.09$. More recent experiments are compatible with zero strangeness [58].

Finally, we compare the results obtained with our models with the BNL E734 experimental data. The mean value of neutrino (antineutrino) energy is 1.3 GeV (1.2 GeV) for BNL experiment, while for MiniBooNE experiment it is 788 MeV (665 MeV). In Figure 6 the differential cross sections evaluated using the RFG, HO+FSI, NO+FSI, SUSA scaling functions, and RMF model are compared with NCQE $\nu p \to \nu p$ [panel (a)] and $\bar{\nu} p \to \bar{\nu} p$ [panel (b)] BNL E734 experimental data. The BNL E734 experiment was performed using a 170-metric-ton high-resolution target-detector in a horn-focused (anti)neutrino at the Brookhaven National Laboratory. The cross sections results show a behaviour similar to those of the MiniBooNE experiment. The latter (using the Cherenkov detector filled with mineral oil (CH_2)) is sensitive to both $\nu(\bar{\nu})p$ and $\nu(\bar{\nu})n$ NCQE scattering [2, 5]. It has been known for some time (see, *e.g.*, [46, 47, 49]) that the Δs-dependence of the NCQE neutrino-nucleon cross section is very mild. This results from a cancellation between the effect of Δs on the proton and neutron contributions, which are affected differently by the axial strangeness: by changing Δs from zero to a negative value the proton cross section gets enhanced while the neutron one is reduced, so that the net effect on the total cross section is very small. NCQE $\nu(\bar{\nu})p$ differential cross sections were measured in the BNL E734 experiment, which are sensitive to the values of Δs (there is not a cancellation effect). The BNL E734 experimental data can be reproduced within our models in principle by the fit of the axial strangeness without change of the axial mass value.

Here we would like to mention that, first, our calculations using NO and HO single-particle wave functions in $n_i(p)$ in the spectral function with FSI and without FSI show that the inclusion of FSI effects leads to a small change (a depletion) of the cross sections. Second, the results for the cross sections obtained using realistic spectral function $S(p, \mathcal{E})$ with single-particle momentum distributions $n_i(p)$ that include Jastrow short-range NN correlations (accounted for in the NO's) are compared in Figures 2 and 6 with those when NN correlation are not included (RFG and HO). It can be seen that, similarly to the case of CCQE neutrino scattering (see Ref. [42]), the differences between results in correlated and non-correlated approaches are small, thus showing that the process is not too sensitive to the specific treatment of the bound state.

4. Conclusions

The main objective of this work is centered in the use of a realistic spectral function, that accounts for short-range NN correlations, and has also a realistic energy dependence. This function gives a scaling function in accordance with the electron scattering data and it can be used for a wide range of neutrino energies. Therefore, the use of this spectral function to describe the general reaction mechanism involved in NC neutrino-nucleus scattering processes can provide very valuable information that can be confronted with results obtained with other theoretical approaches. In this sense, we compare our spectral function-based predictions with the results provided by the SuSA, RMF and RGF models largely used by us in the past. The discrepancies found can help disentangling effects directly linked to particular ingredients in the process: final state interactions, nucleon correlations, effects beyond the impulse approximation, *etc.*

The predictions of our model agree in general with previous results although with some peculiarities that should be emphasized. Our calculations showed that the inclusion of FSI effects in the spectral function-based calculations leads to a slight depletion of the cross section being in a close agreement with the RFG prediction. The inclusion of FSI effects in the RGF model leads to larger cross sections, in good agreement with the data. On the contrary, SuSA and, in particular, RMF approaches lead to significantly smaller differential cross sections at low values of $|Q^2|$ ($\leq$ 0.6–0.8 GeV^2) departing also from the data. This behavior can be seen for the two experiments considered in the work: MiniBooNE and BNL. Another point of relevance when comparing the different models is the softer Q^2 dependence (with a smaller slope) shown by the RMF cross section. Whereas it is clearly below the other curves at low Q^2 (up to $\approx$ 0.5–0.6 GeV^2), it crosses them providing the largest contribution at higher Q^2. This result can be taken as an indication of the particular sensitivity of the NC processes to the specific description of the FSI effects. It may be also connected with the increasing tail in the scaling function provided by the RMF model at larger Q^2-values. This is a consequence of the enhancement of the lower components in the relativistic nucleon wave functions, particularly, for the final state.

All our calculations are based on the impulse approximation, *i.e.*, they do not include effects beyond the one-body approach, for example $2p-2h$ contributions induced by meson exchange currents. These ingredients have been shown to be very important in the analysis of neutrino-nucleus scattering processes. In particular, they produce a significant enhancement in the cross section at low-to-moderate values of the transferred four momentum. This is consistent with our predictions that clearly underestimate data for such kinematical regions. On the contrary, the

agreement is improved at higher Q^2. This is strictly true for neutrinos at MiniBooNE. In the case of antineutrinos, MiniBooNE data at $Q^2 \geq$ 1–1.2 GeV^2 are higher than theoretical predictions, the RMF results being closer to the experiment. More studies are needed in order to understand these differences at medium-large Q^2-values. This could be related to a different role played by $2p-2h$ contributions and MEC for neutrinos and antineutrinos. Work is in progress to evaluate the impact of $2p-2h$ excitations on these results.

Acknowledgements

This work was partly supported by the Bulgarian National Science Fund under Contract No. KP-06-N38/1.

References

[1] A. A. Aguilar-Arevalo *e*t al. (MiniBooNE Collab.), *Phys. Rev. D* **81** (2010) 092005.

[2] A. A. Aguilar-Arevalo *et al.* (MiniBooNE Collab.), *Phys. Rev. D* **82** (2010) 092005.

[3] L. A. Ahrens *et al.*, *Phys. Rev. D* **35** (1987) 785; G. T. Garvey, W. C. Louis, and D. H. White, *Phys. Rev. C* **48** (1993) 761; L. Bugel *et al.* (FINeSSE Collab.), arXiv:hep-ex/0402007; C. Athanassopoulos *et al.* (LSND Collab.) *Phys. Rev. C* **55** (1997) 2078; C. Athanassopoulos *et al.* (LSND Collab.) *Phys. Rev. C* **56** (1997) 2806 (1997); V. Lyubushkin *et al.* [NOMAD Collab.], *Eur. Phys. J. C* **63** (2009) 355.

[4] A. A. Aguilar-Arevalo *et al.* (MiniBooNE Collab.), *Phys. Rev. D* **88** (2013) 032001.

[5] A. A. Aguilar-Arevalo *et al.* (MiniBooNE Collab.), *Phys. Rev. D* **91** (2015) 012004.

[6] A. M. Ankowski, *Phys. Rev. C* **86** (2012) 024616.

[7] P. Lipari, *Nucl. Phys. B, Proc. Suppl.* **112** (2002) 274; G. P. Zeller, arXiv:hep-ex/0312061.

[8] A. Meucci, C. Giusti and F. D. Pacati, *Phys. Rev. D* **84** (2011) 113003.

[9] A. V. Butkevich and D. Perevalov, *Phys. Rev. C* **84** (2011) 015501.

[10] O. Benhar and G. Veneziano, *Phys. Lett. B* **702** (2011) 433.

[11] M. Martini, M. Ericson and G. Chanfray, *Phys. Rev. C* **84** (2011) 055502.

[12] J. Nieves, I. R. Simo and M. J. V. Vacas, *Phys. Lett. B* **707** (2012) 72.

[13] J. E. Amaro *et al.*, *Phys. Rev. D* **84** (2011) 033004.

[14] A. Meucci *et al.*, *Phys. Rev. Lett.* **107** (2011) 172501.

[15] V. Bernard, L. Elouadrhiri and Ulf-G Meißner, J. Phys. G **28**, R1 (2002).

[16] M. Martini *et al.*, *Phys. Rev. C* **80** (2009) 065501.

[17] M. Martini *et al.*, *Phys. Rev. C* **81** (2010) 045502.

[18] R. Gonzalez-Jimenez *et al.*, *Phys. Rev. C* **88** (2013) 025502.

[19] R. González-Jiménez *et al.*, *Phys. Lett. B* **718** (2013) 1471.

[20] M. V. Ivanov *et al.*, *Phys. Lett. B* **727** (2013) 265.

[21] A. Meucci and C. Giusti, *Phys. Rev. D* **89** (2014) 057302.

[22] A. Meucci *et al.*, *Phys. Rev. C* **80** (2009) 024605.

[23] A. Meucci and C. Giusti, *Phys. Rev. D* **85** (2012) 093002.

[24] J. E. Amaro *et al.*, *Phys. Rev. C* **71** (2005) 015501.

[25] J. E. Amaro *et al.*, *Phys. Rev. Lett.* **98** (2007) 242501.

[26] D. B. Day *et al.*, *Annu. Rev. Nucl. Part. Sci.* **40** (1990) 357.

[27] I. Sick, D. B. Day, and J. S. McCarthy, *Phys. Rev. Lett.* **45** (1980) 871.

[28] C. Ciofi degli Atti *et al.*, *Phys. Rev. C* **36** (1987) 1208; *Phys. Rev. C* **39** (1989) 259; *Phys. Rev. C* **43** (1991) 1155; *Phys. Rev. C* **46** (1992) 1045; *Phys. Rev. C* **53** (1996) 1689; *Phys. Lett. B* **458** (1999) 447.

[29] W. M. Alberico *et al.*, *Phys. Rev. C* **38** (1988) 1801.

[30] M. B. Barbaro *et al.*, *Nucl. Phys. A* **643** (1998) 137.

[31] T.W. Donnelly and I. Sick, *Phys. Rev. Lett.* **82** (1999) 3212.

[32] T.W. Donnelly and I. Sick, *Phys. Rev. C* **60** (1999) 065502.

[33] C. Maieron *et al.*, *Phys. Rev. C* **65** (2002) 025502.

[34] M. B. Barbaro *et al.*, *Phys. Rev. C* **69** (2004) 035502.

[35] A.N. Antonov *et al.*, *Phys. Rev. C* **69** (2004) 044321; *Phys. Rev. C* **71** (2005) 014317; *Phys. Rev. C* **73** (2006) 047302; *Phys. Rev. C* **74** (2006) 054603.

[36] M.V. Ivanov *et al.*, *Phys. Rev. C* **77** (2008) 034612.

[37] I. Ruiz Simo *et al.*, *Phys. Rev. D* **97** (2018) 116006.

[38] J.E. Amaro *et al.*, *Phys. Lett. B* **696** (2011) 151.

[39] O. Lalakulich *et al.*, *Phys. Rev. C* **86** (2012) 014614.

[40] G.D. Megias *et al.*, *Phys. Rev. D* **94** (2016) 093004.

[41] K. Abe *et al.*, *Phys. Rev. Lett.* **56** (1986) 1107; **56** (1986) 1883(E); L.A. Ahrens *et al.*, *Phys. Rev. D* **35** (1987) 785.

[42] M.V. Ivanov *et al.*, *Phys. Rev. C* **89** (2014) 014607.

[43] M.V. Ivanov *et al.*, *Phys. Rev. C* **99** (2019) 014610.

[44] J.E. Amaro *et al.*, *Phys. Rev. C* **73** (2006) 035503.

[45] M. C. Martinez *et al.*, *Phys. Rev. C* **73** (2006) 024607.

[46] M. B. Barbaro *et al.*, *Phys. Rev. C* **54** (1996) 1954.

[47] W. M. Alberico *et al.*, *Nucl. Phys. A* **623** (1997) 471.

[48] M. C. Martinez *et al.*, *Phys. Rev. C* **77** (2008) 064604.

[49] W. M. Alberico *et al.*, Nucl. Phys. A **651** (1999) 277.

[50] M.V. Ivanov *et al.*, *Phys. Rev. C* **91** (2015) 034607.

[51] M.C. Martinez *et al.*, *Phys. Rev. Lett.* **100** (2008) 052502.

[52] F. Capuzzi *et al.*, *Nucl. Phys. A* **524** (1991) 681.

[53] A. Meucci *et al.*, *Phys. Rev. C* **67** (2003) 054601.

[54] A. Meucci *et al.*, *Phys. Rev. C* **83** (2011) 064614.

[55] E.D. Cooper *et al.*, *Phys. Rev. C* **80** (2009) 034605.

[56] D. Perevalov, *Neutrino-nucleus neutral current elastic interactions measurement in MiniBooNE* (2009) PhD Thesis, University of Alabama, United States.

[57] http://www-boone.fnal.gov/for_physicists/data_release/ncel

[58] S. F. Pate and J. P. Schaub, *J. Phys. Conf. Ser.* **295** (2011) 012037.